occurred, which is characterized by the approach and separation of the two vibrational levels and a concomitant intensity transfer from ν_D to ν_S. Above this point, the frequency of the stretching vibration exceeded the deformational mode (Fig. 4), indicating that proton tunneling between two potential minima has been suppressed, which is consistent with the presence of static, symmetric hydrogen bonds (*24*). Further information on the structure, including changes in hydrogen positions and possible distortion of the O sublattice, will be possible if synchrotron x-ray measurements on ice are made in this newly accessible pressure range.

REFERENCES AND NOTES

1. Ph. Pruzan, *J. Mol. Struct.* **322**, 279 (1994).
2. W. B. Holzapfel, *J. Chem. Phys.* **56**, 712 (1972).
3. F. H. Stillinger and K. S. Schweitzer, *J. Phys. Chem.* **87**, 4281 (1983).
4. C. Lee, D. Vanderbilt, K. Laasonen, R. Car, M. Parrinello, *Phys. Rev. Lett.* **69**, 462 (1992); *Phys. Rev. B* **47**, 4863 (1993).
5. P. Demontis, R. LeSar, M. L. Klein, *Phys. Rev. Lett.* **60**, 2284 (1989); *Phys. Rev. B* **40**, 2716 (1989).
6. J. Hama, K. Suito, M. Watanabe, *High Pressure Research in Mineral Physics: Application to Earth and Planetary Sciences* (Terra Scientific, Tokyo—American Geophysical Union, Washington, DC 1992), p. 403.
7. M. Benoit, M. Bernasconi, P. Focher, M. Parrinello, *Phys. Rev. Lett.* **76**, 2934 (1996).
8. Ph. Pruzan, J. C. Chervin, M. Gauthier, *Europhys. Lett.* **13**, 81 (1990); Ph. Pruzan, J. C. Chervin, B. Canny, *J. Chem. Phys.* **99**, 9842 (1993).
9. A. Polian and M. Grimsditch, *Phys. Rev. Lett.* **52**, 1312 (1984).
10. K. R. Hirsch and W. B. Holzapfel, *J. Chem. Phys.* **84**, 2771 (1986).
11. R. J. Hemley *et al.*, *Nature* **330**, 737 (1987). More recent x-ray diffraction measurements to pressures have revealed additional structural information but are consistent with the persistence of a structure based on bcc oxygen (M. Somayazulu *et al.*, unpublished results; Ph. Pruzan *et al.*, *European Synchrotron Radiation Facility Annual Report, 1994–1995*, p. 12; P. Loubeyre, personal communication).
12. R. J. Nelmes *et al.*, *Phys. Rev. Lett.* **71**, 1192 (1993); J. M. Besson *et al.*, *Phys. Rev. B* **49**, 12540 (1994).
13. M. E. Lines and A. M. Glass, *Principles and Applications of Ferroelectrics and Related Materials* (Clarendon Press, Oxford, 1977), p. 32.
14. D. D. Klug and E. Whalley, *J. Chem. Phys.* **81**, 1220 (1984).
15. K. Aoki, H. Yamawaki, M. Sakashita, *Science* **268**, 1322 (1995).
16. ———, *Phys. Rev. Lett.* **76**, 784 (1996).
17. We performed the measurements on the U2B IR beam line at the National Synchrotron Light Source (NSLS), using a Fourier transform–IR (Nicolet 750) spectrometer with KBr beam splitter. The characteristics of the beam line are given by G. L. Carr *et al.* [*Rev. Sci. Instrum.* **66**, 1643 (1995)]. Synchrotron light passes through the spectrometer and is focused into the diamond anvil cell to spots 20 to 30 μm in diameter (in the visible), using a custom-built IR microscope with Cassegrain mirror objective (numerical aperture = 0.25, ×8). For absorption measurements, a ZnSe lens placed inside a Mao-Bell diamond-anvil cell collects the light transmitted through the sample and images it on a mercury-cadmium telluride detector (MCT). Reflected light is collected by the same mirror objective, which illuminates the sample, applying a half-mirror beam splitter. A separate MCT detector was used to record the reflectivity, which permitted collection of complementary absorption and reflectivity spectra at each pressure.
18. From Kramers-Kronig transformation of the reflectivity spectra, we can obtain both the real and the imaginary parts of the dielectric function, $\epsilon_1 + i\epsilon_2$ [F. C. Jahoda, *Phys. Rev.* **107**, 1261 (1957)]. In contrast, there is no regular procedure to derive both ϵ_1 and ϵ_2 from absorption measurements.
19. H. K. Mao, J. Xu, P. M. Bell, *J. Geophys. Res.* **91**, 4673 (1986).
20. R. J. Hemley, H. K. Mao, A. F. Goncharov, M. Hanfland, V. V. Struzhkin, *Phys. Rev. Lett.* **76**, 1667 (1996).
21. V. V. Struzhkin, A. F. Goncharov, M. Somayazulu, R. J. Hemley, H. K. Mao, in preparation.
22. We used a standard oscillator model (*25*) for each of the observed bands, as well as a Kramers-Kronig transformation procedure to relate the absorption and reflectivity spectra (*21*). Between 60 and 80 GPa, the inclusion of at least three oscillators is required to account for the observed spectra in the lower frequency range. The lowest frequency oscillator (ν_S) has the greatest strength and is below the measured spectral range (<600 cm^{-1}). We believe that this band originates from the stretching mode of the low-pressure phase. A narrow band at 1300 cm^{-1} (ν_D) is a deformational mode of the O–H bond related to the rotational band ν_R of the low-pressure phase. The pressure dependence of the frequency of this band shows a change in slope at 60 GPa. Only those two modes are IR-allowed for the ice X structure. The third weak, broad band is close to the position of stretching mode of the low-pressure phase ν_3' near the transition point (*21*). The independent oscillator fit to the reflectivity spectra in this pressure-frequency range was not sufficient to model the data, and we obtained much better fits when we included an interaction between stretching and rotational mode as suggested (*23*). Two interacting oscillators were sufficient to fit the reflectivity spectra above 80 GPa. Aoki *et al.* (*16*) interpreted absorption near 1200 cm^{-1} as a Fano-type interference between a narrow band and the continuum. We find, however, that the observed line shape does not necessarily require interference, because two independent oscillators (the first, a relatively weak and narrow IR band inside a second, the strong and broad reststrahlen band) also give rise to a Fano-like absorption as a result of the complex behavior of the optical constants (*21*).
23. Alternatively, calculations using a double-well potential model for the hydrogen bond suggest that this could also arise from splitting of energy levels associated with the changing barrier height (*21*).
24. The double-well potential calculations also predict a change in proton motion at these pressures (*21*). Although the spectroscopic features at 150 to 160 GPa are indicative of a type of Fermi resonance, a second phase transition cannot be ruled out.
25. A. S. Barker and J. J. Hopfield, *Phys. Rev. A* **135**, 1732 (1964).

26. We are grateful to P. Loubeyre, Ph. Pruzan, and J.-M. Besson for comments on the manuscript. This work was supported by the National Science Foundation and NASA. The NSLS is supported by the Department of Energy under contract DE-AC02-76-CH00016.

20 March 1996; accepted 8 May 1996

Making DNA Add

Frank Guarnieri, Makiko Fliss, Carter Bancroft*

Recent studies have demonstrated the feasibility of using DNA-based experiments to compute solutions to combinatorial problems. However, a prerequisite for designing a computer useful in a wide range of applications is the ability to perform mathematical calculations. The development of a DNA-based algorithm for addition is presented. The DNA representation of two nonnegative binary numbers is presented in a form permitting a chain of primer extension reactions to carry out the addition operation. To demonstrate the feasibility of this algorithm, a simple example was executed biochemically.

In a pioneering study, Adleman used DNA to solve a directed Hamiltonian path problem (*1*), thus demonstrating the feasibility of a molecular approach to the solution of combinatorial problems. This approach has been extended by Lipton to the solution of another NP-complete problem, the "satisfaction" problem (*2*). These elegant studies demonstrated how problems corresponding to Boolean formulas can be solved by a massively parallel processing procedure that makes use of the ability of DNA sequences to hybridize specifically to their complementary sequences. More recently, Reif has proposed an abstract mathematical model for the performance of parallel molecular computation (*3*).

It is clearly of interest to design DNA-based computers capable of performing search procedures. However, design of a versatile computer requires development of the bit manipulations for carrying out addition. Mathematical calculations such as addition represent a different problem than the solution of search problems. A search problem can be solved by generating all possible combinations and searching for the correct output, whereas binary operations such as addition require that only the correct output is produced in response to specific inputs. Consequently, the addition operation requires a quite different model for the use of DNA in computing than that used previously for search procedures. As an approach to the development of a generally

Department of Physiology and Biophysics, Mount Sinai School of Medicine, One Gustave L. Levy Place, New York, NY 10029, USA.

*To whom correspondence should be addressed at Department of Physiology and Biophysics, Box 1218, Mount Sinai School of Medicine, One Gustave L. Levy Place, New York, NY 10029, USA. E-mail: cbancro@smtplink.mssm.edu

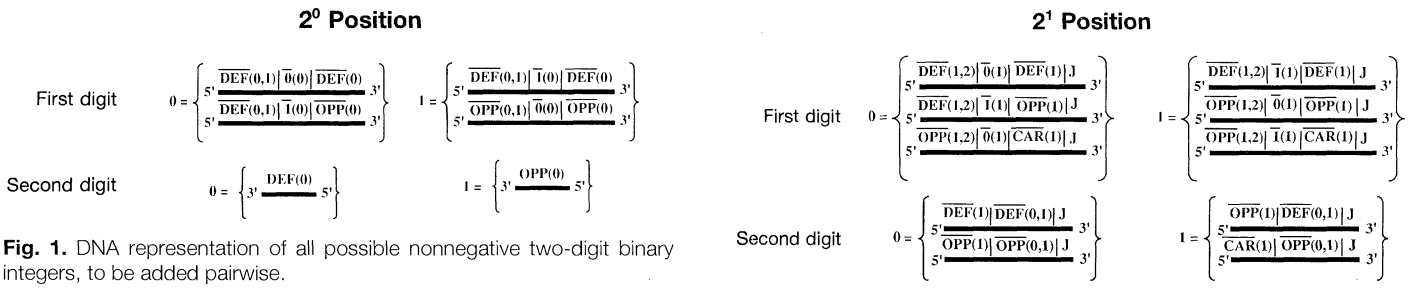

Fig. 1. DNA representation of all possible nonnegative two-digit binary integers, to be added pairwise.

useful DNA-based computer, we have generated and applied a paradigm for making DNA add any two rational nonnegative binary numbers.

We first present a general algorithm for DNA-based addition of any two nonnegative rational binary numbers. We begin with the DNA representation of all possible pairs of input nonnegative two-digit integers (Fig. 1). The "first digit" and "second digit" at a given 2^n position refer to the value (either 0 or 1) at that position of, respectively, the first and second numbers to be added. All DNA sequences are single-stranded, unique, and noncomplementary, except that overlining indicates a complementary DNA sequence [for example, $\overline{\text{DEF}}(0, 1)$ is complementary to DEF(0, 1)]. A number in parentheses refers to a position, whereas a number not in parentheses refers to the value of the digit at that position. The first digit at the 2^0 position is represented by two DNA strands, each containing (from the 5′ end) a "position transfer operator" [for example, $\overline{\text{DEF}}(0, 1)$, which transfers information from the 2^0 to the 2^1 position], an element representing the value of the digit at the 2^0 position, and a "position operator" [for example, $\overline{\text{DEF}}(0)$, which is used only at the 2^0 position]. The second digit at the 2^0 position is represented by a single DNA strand with the sequence DEF or OPP if the digit is, respectively, 0 or 1. This strand represents an operator that will serve as a primer in a primer extension reaction (4). The second digit at the 2^1 position is represented by two DNA strands, each containing a position transfer operator [either $\overline{\text{DEF}}(0, 1)$ or $\overline{\text{OPP}}(0, 1)$ as above or a third operator, termed $\overline{\text{CAR}}(0, 1)$ ("Carrier")], a position operator, and a J element that will prevent template extension. Only one of the strands representing this digit will serve as a template for further elongation of the result strand. If a 0 or 1 were carried from the reaction at the 2^0 position, the primer extension template would be, respectively, the first or second strand of this digit. Thus, the roles of the position transfer operators in the representation of the 2^0 position and the 2^1 position are, respectively, to send and receive information. The first digit at the 2^1 position is represented by three strands, each containing the indicated four elements, defined as above. Only one of these strands will serve as a primer for continued extension of the result strand, as follows: If the reaction at the 2^0 position brought to the 2^1 position a 0 and the value of the second digit at the 2^1 position is a 0 or 1, then the template is, respectively, the appropriate first or second strand. However, if the 2^0 reaction brought to the 2^1 position a 1 and the value of the second digit at the 2^0 position is also a 1, then the template is the third strand representing the value 1, and in addition a 1 must be "carried" to the 2^2 position. To permit this final information transfer, a placeholder strand for the 2^2 position is included, which will serve as a template to further extend the result DNA strand only under appropriate conditions. The latter operations are analogous to the "bit flipping" used in electronic computers.

As a schematic example, we illustrate the use of this algorithm to add binary 11 + 01 (Fig. 2). The input DNAs for each of the four reactions illustrated are as follows: the first and second input 2^0 position digits (each = 1), the second digit at the 2^1 position (0), the first digit at the 2^1 position (1), and the placeholder strand. In reaction 1, the operator (primer) representing the second digit at the 2^0 position hybridizes to the appropriate strand representing the first digit at the 2^0 position and, upon primer extension, yields result strand 1 (RS1), encoding a 0 at the 2^0 position. In reaction 2, RS1 hybridizes to the appropriate strand of the second digit at the 2^1 position, yielding, after extension of RS1, RS2. In reaction 3, RS2 primes the appropriate strand of the first digit at the 2^1 position, resulting in extension of RS2 to yield RS3, now additionally encoding a 0 at the 2^1 position. Finally, in reaction 4, RS3 primes the placeholder strand for the 2^2 position, resulting in extension of RS3 to yield the final result strand. These successive reactions together represent an example of a process we term a horizontal chain reaction, in which input DNA sequences serve as successive tem-

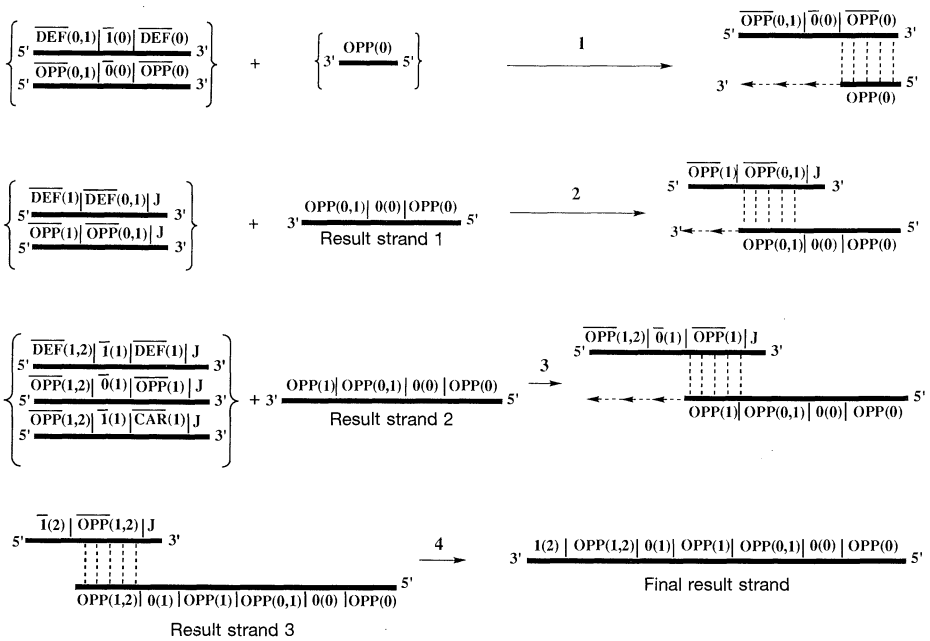

Fig. 2. Illustration of the operation 11 + 01 as an example of a DNA-based algorithm for adding two two-digit binary numbers. Vertical dotted lines represent hybridization between complementary DNA elements, and reiterated arrows represent primer extension.

plates for extension of a result strand. The final result strand encodes three digits, interspersed with operator sequences, that represent precisely and in the correct order the outcome of the addition operation: 100. In addition, each such element encodes both the value and position of a result digit. A number of molecular biological approaches could thus be applied to the readout operation; for example, use of appropriate oligomers as hybridization probes or polymerase chain reaction (PCR) primers, or direct DNA sequencing (4).

Generalization of this algorithm to the addition of two nonnegative n-digit binary numbers is straightforward. If necessary, zeroes are added to the left of the smaller integer so that both numbers are represented by the same number of digits. The two digits in the 2^0 position are represented as in Fig. 1. The two digits in each of the positions 2^1 through 2^n are represented as shown for the 2^1 position in Fig. 1, with the following modification. At a position i other than 1, unique DNA sequences represent the values $0(i)$ and $1(i)$, and operators are replaced appropriately; for example, $\overline{\mathrm{DEF}}(1)$ and $\overline{\mathrm{DEF}}(1, 2)$ by DNA sequences representing $\overline{\mathrm{DEF}}(i)$ and $\overline{\mathrm{DEF}}(i, i + 1)$. Finally, a placeholder DNA strand with the sequence 5′ $\overline{1}(n + 1)/\overline{\mathrm{OPP}}(n, n + 1)/\mathrm{J}$ 3′ is included. The addition operation is in theory exactly as described above. This operation will yield a final result strand longer than that shown in Fig. 2, but with the same basic structure; that is, elements representing in the correct order the numerical outcome of the operation, interspersed with operator sequences. This more general algorithm can readily be extended to the addition of any two n-digit positive rational numbers (5).

We have designed and executed an application of our algorithm to DNA-based addition of all possible pairs of nonnegative binary integers. Addition is performed by combining in a test tube primer extension reagents plus the DNA strands appropriately representing the two numbers to be added, followed by a primer extension reaction (6). The predicted reactions are illustrated in Fig. 3 (because only the 2^0 position is represented, neither the position transfer operators nor the position indicators defined above for the general algorithm are needed). For 0 + 0, the 20-base input operator DEF hybridizes specifically to the 40-base "defining" (first input digit) strand, and primer extension elongates the DEF operator to yield a 40-base result strand encoding DEF plus the result 0. For 0 + 1, the 20-base input operator OPP hybridizes to the 70-base "opposite" strand, yielding after primer extension a 70-base result strand encoding OPP plus the result 1. Similarly, input of 1 + 0 yields a 70-base result strand encoding DEF plus the result 1. For 1 + 1 (= 10 in binary notation), the first primer extension reaction (Fig. 3A) yields the 60-base first result strand and transforms the potential primer creator $\overline{\mathrm{PP}}$ into the actual primer PP. Consequently (Fig. 3B), the placeholder strand functions as a template for further extension of this result strand, yielding a 110-base result strand. This result strand contains a 0 written in the 2^0 position and a 1 that has been carried to the 2^1 position. Thus, the placeholder strand has yielded transfer of information from the 2^0 to the 2^1 position, generating a final result strand directly encoding the outcome of the addition operation, 10 (in binary). This is the simplest example of the horizontal chain reaction described above.

This simple theoretical algorithm was executed biochemically (6). Figure 4A shows that the 0 + 0 operation yielded the expected 40-base-long result strand, whereas the operations 0 + 1 and 1 + 0 each yielded the expected 70-base-long result strand, thus satisfying biochemically the required commutativity of addition. Similar results for the latter two operations were obtained in a separate reaction (Fig. 4B), although for reasons not presently clear, the 1 + 0 result strand migrated slightly faster than predicted. Figure 2B also shows that the operation 1 + 1 yielded the expected 110-base-long result strand, demonstrating that both of the successive reactions illustrated in Fig. 1, A and B, for this operation had occurred. These results demonstrate the biochemical execution of the addition algorithm depicted in Fig. 3. In particular, the successful performance of the 1 + 1 operation demonstrates experimentally that a placeholder DNA strand can be used to extend a single-digit DNA algorithm to one in which a second binary digit is incorporated into the calculation.

Use of the general algorithm (Fig. 1) to add two large binary numbers may require some technical modifications. As the number of successive primer extension reactions increases, the possibility of errors in both these reactions and the readout process will increase. The introduction of redundant steps or increased hybridization stringency (or both) may be useful in overcoming this prob-

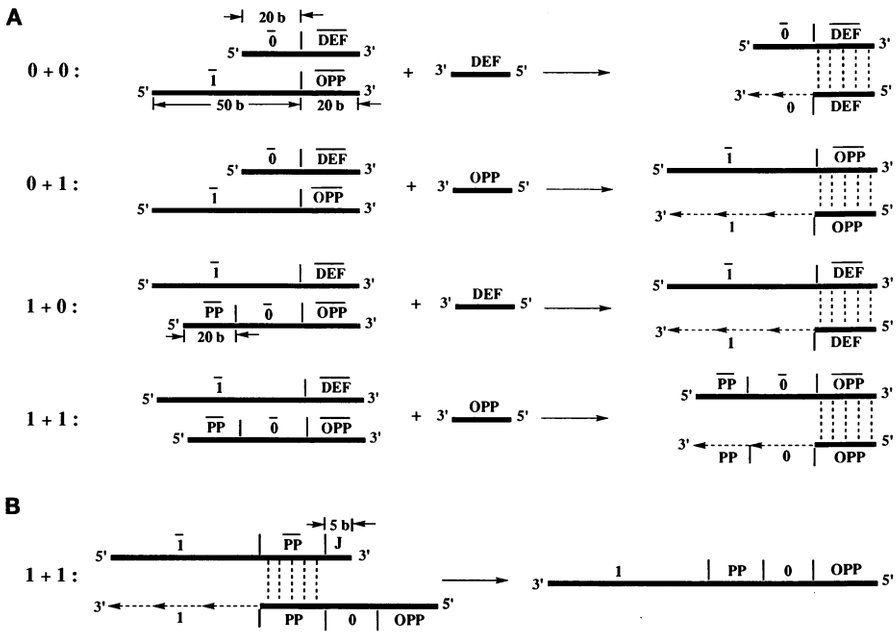

Fig. 3. Illustration of a simple DNA-based algorithm for adding two binary digits. (**A**) Input DNA strands and expected reactions for the operations 0 + 0, 0 + 1, and 1 + 0, and input DNA strands and expected first reaction in the 1 + 1 operation. (**B**) Input placeholder DNA strand and expected second reaction in the 1 + 1 operation. Vertical dotted lines and reiterated arrows are as in Fig 2.

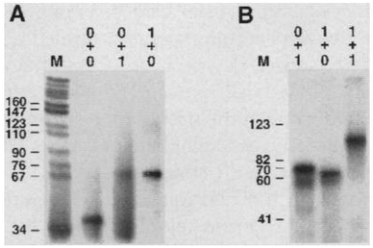

Fig. 4. Biochemical execution of a simple DNA-based algorithm for adding two binary digits. M, single-stranded molecular size markers. Molecular sizes are indicated on the left (in bases). (**A**) Products of each of the first three addition reactions shown in Fig. 3A. (**B**) Products of the (0 + 1) and the (1 + 0) reactions (Fig. 3A) and the sequential (1 + 1) reactions (Fig. 3, A and B).

lem. Also, cumulative effects of inefficiencies in each of the primer extension reactions may necessitate that the growing result DNA strand be isolated, possibly amplified by PCR, and the reaction continued in a new test tube or tubes containing components required for the remaining steps in the algorithm.

The first generation addition algorithm described here has an obvious limitation. Because the output is encoded in a different form than the input, it is not presently possible to perform either iterative or parallel addition. The development of a more mature DNA-based addition algorithm will require modification of the present procedure to take full advantage of the enormous potential of DNA to engage in massively parallel reactions.

Other aspects of the present algorithm deserve comment: (i) The operator corresponding to the second digit at the 2^0 position plays a special role, because no primer extension reaction would occur without this DNA strand. This operator thus initiates a horizontal chain reaction, involving multiple sequential reactions that ultimately yield the final result strand (*7*). (ii) The amount of DNA required to perform this algorithm does not rise exponentially with the number of digits n in each of the two numbers to be added, but is only a linear function of n. For large n, where end effects of the 2^0 position and the placeholder strand can be ignored, representation of each of the two numbers to be added requires $2.5n$ DNA strands. (iii) The algorithm described here is not technically demanding, because the simple biochemical procedures involved require approximately 1 or 2 days of laboratory work.

Finally, a distinctive aspect of this algorithm is the production in each reaction of a successively elongated result DNA strand that serves a dual function in the addition operation. One role of the result strand is to record, in the proper order, the result of each reaction in the operation. In this sense, the growing result strand is analogous to a passive tape on which the outcome of successive operations is written, yielding finally an output tape that encodes the result of the addition operation. However, the growing result strand is also an active participant in the addition algorithm because the output result strand for each operation (reaction) serves as the operator (primer) for the succeeding operation. Thus, the result DNA strand serves both as an operator that transfers information during the addition algorithm and as a tape that records the outcome of this algorithm.

REFERENCES AND NOTES

1. L. M. Adleman, *Science* **266**, 1021 (1994).
2. R. J. Lipton, *ibid.* **268**, 542 (1995).
3. J. H. Reif, in *Seventh Annual ACM Symposium on Parallel Algorithms and Architectures (SPAA95)*, Santa Barbara, CA, June 1995, pp. 213–223.
4. F. M. Ausubel *et al.*, Eds., *Short Protocols in Molecular Biology* (Wiley, New York, ed. 3, 1995).
5. F. Guarnieri and C. Bancroft, in *Proceedings of the Second Annual Meeting on DNA Based Computers*, Princeton, NJ, 10 to 12 June 1996 (American Mathematical Society, Providence, RI, in press).
6. The elements illustrated in Fig. 3 were represented by the following sequences (all listed 5′ to 3′) or the appropriate complementary sequence (or both): $\overline{O}$, CCTTACCCCTTTCTACCTCT; DEF, TCGTCTCAGGGGGGGTGCTT; $\overline{1}$, CACGAAACGAGCGAAAGCACCCACAACAAGAACCACACAGCACAACCAGA; OPP, GACCAAATACAGGCTAACAT; $\overline{PP}$, CATTCCCCTTCCTCTCCTCC; and J, TCTCC. Each primer extension reaction indicated in Fig. 3A was performed by first combining the following reagents in a final volume of 30 μl: supplemented extension buffer [AmpliTaq buffer (Perkin-Elmer), supplemented with 2.5 U AmpliTaq enzyme, 2.5 mM $MgCl_2$, deoxyadenosine triphosphate (dATP) and deoxythymidine triphosphate (dTTP) (each 0.2 mM)], [^{32}P]deoxycytidine triphosphate (dCTP) and [^{32}P]deoxyguanosine triphosphate (dGTP) (each 3000 Ci/mmol), and two DNA strands representing the first number (50 ng each) plus 5 μg of the second number strand. Then for primer extension, reactions were processed for 15 cycles each at 95°C for 1 min, 58°C for 1 min (except for 0 + 1, at 66°C for 1 min), and 72°C for 20 s. Except for 1 + 1, the primer extension reactions indicated in Fig. 3B were the same, except that the [^{32}P]dCTP plus the other three unlabeled deoxynucleotide triphosphates were present. The first 1 + 1 reaction (indicated in Fig. 3A) was also done as described above, except that only dATP, dTTP, and dGTP were present (note that the extended sequence should contain no Cs). After this reaction, 3 μl of the reaction were combined with 5 μg of the 5′ 1/$\overline{PP}$/J 3′ DNA strand (Fig. 3B) [brought to a total volume of 30 μl with supplemented extension buffer as described above (but also containing dGTP)] and [^{32}P]dCTP and subjected to primer extension as above. For all reactions indicated in Fig. 3, samples were then denatured and analyzed by standard denaturing gel electrophoresis [J. Sambrook, E. F. Fritsch, T. Maniatis, *Molecular Cloning* (Cold Spring Harbor Laboratory, Cold Spring Harbor, NY, ed. 2, 1989), p. 13.45)], except that the sample buffer contained in addition 10 mM NaOH. For the analysis shown in Fig. 4, the following denatured (and therefore single-stranded) ^{32}P-labeled molecular size markers were used: (A) Msp I–digested plasmid pBR322; (B) strands $\overline{PP}$/$\overline{O}$/$\overline{OPP}$ and $\overline{1}$/$\overline{DEF}$ (60 and 70 bases, respectively) plus oligomers of the 41 base–long 1P element [G.-Z. Yan, W. T. Pan, C. Bancroft, *Mol. Endocrinol.* **5**, 535 (1991)]. Differences in the efficiencies of individual primer extension reactions were corrected for by applying approximately equal amounts of product. After electrophoresis, the gel was fixed, dried, and imaged by autoradiography and scanning.
7. The horizontal chain reaction described here may find application in a number of areas of computation; for example, in the development of a one-dimensional DNA cellular automaton. We are currently investigating how the horizontal chain reaction concept may be used to develop a DNA-based simulation of a Turing machine.

8. Supported by funds provided by The Mount Sinai School of Medicine. We thank an anonymous reviewer for helpful comments on the manuscript.

26 March 1996; accepted 3 May 1996

Maya Blue Paint: An Ancient Nanostructured Material

M. José-Yacamán,* Luis Rendón, J. Arenas, Mari Carmen Serra Puche

Maya blue paint was often used in Mesoamerica. The origin of its color and its resistance to acids and biocorrosion have not been fully understood. High-resolution transmission electron microscopy, electron energy loss spectroscopy, and x-ray microanalysis studies of authentic samples show that palygorskite crystals in the paint form a superlattice that probably occurs as a result of mixing with indigo molecules. An amorphous silicate substrate contains inclusions of metal nanoparticles encapsulated in the substrate and oxide nanoparticles on the surface. The beautiful tone of the color is obtained only when both the particles and the superlattice are present.

When studying Mayan archeological sites, researchers are always stunned by the blue color often used in pottery, murals, and ceremonial artifacts. The color first described in the Chichén Itza ruins by Merwin (*1*) was named Maya blue by Gettens (*2*). This color differs from any blue ever identified on ancient or medieval paintings from Europe or Asia. It is not based on copper or on ground lapis lazuli or lazurite, which are common in European and Asian paintings (*3*). Maya blue was used in Mesoamerica and colonial Mexico probably as late as the 20th century (Fig. 1). In addition to its beautiful look, Maya blue is resistant to diluted mineral acids, alkalis, solvents, oxidants, reducing agents, moderate heat, and even biocorrosion. Paintings in the Bonampak archeological site have retained their blue color after centuries in the extreme conditions of the rain forest.

The structure of the material and the origin of the Maya blue color have been debated extensively. Maya blue contains clays (mainly palygorskite mixed with

M. José-Yacamán and L. Rendón, Instituto de Física, Universidad Nacional Autónoma de México, Apdo. Postal 20-364, Delegación Alvaro Obregón, 01000 México, D.F., México.
J. Arenas, Instituto Nacional de Investigaciones Nucleares, Carr. México-Toluca Km. 36.5, 52045 Salazar Edo. de México.
M. C. Serra Puche, Museo Nacional de Antropología, Instituto Nacional de Antropología e Historia, Paseo de la Reforma y Gandhi s/n, Polanco, 11560 México, D.F., México.

*To whom correspondence should be addressed. E-mail: yacaman@sysul1.ifisicacu.unam.mx